J. Earth Syst. Sci. (2020)129 66
https://doi.org/10.1007/s12040-019-1329-9

Simulation of coastal aquifer using mSim toolbox and COMSOL multiphysics

Sruthi S Kumar, S Deb Barma* and Mahesha Amai

Department of Applied Mechanics and Hydraulics, National Institute of Technology Karnataka, Surathkal, Mangalore 575025, India.
**Corresponding author. e-mail: surajitdb@gmail.com*

MS received 2 July 2019; revised 20 October 2019; accepted 31 October 2019

Fluctuations in groundwater levels along the coast have a significant impact on the extent of saltwater intrusion into freshwater aquifers. This study aims to simulate the groundwater flow and solute transport in the region by using the mSim toolbox in the MATLAB and COMSOL Multiphysics. The investigation is focussed on a micro-basin of Pavanje river located along the west coast of India. The model results are calibrated and validated against the field observations. The results show that the variation of the water table over the year is significant and range from about 3–14 m. There exists a reasonable correlation between the simulated and observed values of groundwater level and salinity. The wells that are most vulnerable to seawater intrusion in the region are identified. The COMSOL model estimated a salinity range of 0–20 mol/m^3. Additionally, the model is used to understand the response of coastal aquifer to various stress scenarios. The study reveals that reduced recharge rate with increased pumping has a serious impact on aquifer system.

Keywords. Coastal aquifers; COMSOL Multiphysics; MATLAB; mSim; predictive simulation; saltwater intrusion.

List of symbols

$\xi = \xi(x, y)$	The distance between the reference level and the saltwater–freshwater interface
$b = b(x, y)$	The total freshwater head, applicable to both zones of the aquifer $= h_f$ for zone 1; $b(x, y) = h_f - d + \xi(x, y)$ for zone 2
h_f	Freshwater head concerning the aquifer base
N	Aquifer recharge rate, which replenishes the aquifer
τ	Intersection between the interface and the base of the aquifer, which is usually called "toe" of the seawater wedge

The hydraulic head h_f and the variable ξ are related through the following equation $(1/\varepsilon)(h_f - d) = \xi(x, y)$, in which ε is the density ratio $\varepsilon = (\rho_0 - \rho_s)/\rho_0$, where ρ_s stands for the maximum seawater density

1. Introduction

The coastal groundwater resources are critical component of the available freshwater along the sea coast. The enhanced dependencies and over-extraction on coastal aquifer have resulted in groundwater depletion leading to saltwater intrusion. Unplanned exploitation of freshwater aquifers

Published online: 07 February 2020

has led to severe groundwater quality problems worldwide. This problem is predominant in the coastal aquifer system, as the coastal groundwater systems are sensitive to impacts such as decreased recharge, contamination from natural and human-made sources and over-exploitation (Essink 2001) considering the threat of seawater intrusion. Under natural conditions, there exists an equilibrium between saltwater and freshwater due to seaward freshwater gradient resulting in nominal saltwater intrusion into freshwater aquifer. Due to excessive pumping, seaward freshwater gradient gets reduced and even sometimes may be reversed to the landward direction. This leads to aggressive saltwater intrusion from the sea contaminating inland freshwater aquifers to a large extent, which may take several years to get remediated (Werner 2010). To address this issue effectively, density-dependent groundwater model is required to track the movement of the solute in coastal aquifers (Lin *et al.* 2009). The prediction of distribution and concentration of contaminants across the groundwater–surface water interface (GWSWI) was reported by Bobba (2012).

The Dakshina Kannada district which is the coastal district of Karnataka spreads along the west coast of India covering coastal track of about 30 km. Agriculture and fishing are the main occupation of people in this area. However, due to the developmental activities and urbanisation in recent years, mainly in the fields of industry, commerce and trade, the demand for fresh water has enormously increased (Priyanka *et al.* 2018). The groundwater extraction changes the dynamic balance between the flow of freshwater and the saltwater–freshwater interface so that the interface will advance further and attain an equilibrium position governed by the quantity extracted and the balance outflow of freshwater to the sea. When the groundwater withdrawals are significant from the locations close to the saltwater interface, the saltwater upcoming may rise to the screened section of wells and turn the water saline. Under the above circumstance, it is very much essential to consider the effective and optimal utilisation of coastal aquifer for freshwater supply (Mantoglou 2003; Kourakos and Mantoglou 2013). Given that withdrawals from the aquifer system can affect the water levels, water quality, coastal discharge and surface water–groundwater interactions, a better understanding of the groundwater flow system of the study area is needed for effective water resources management (Mantoglou 2003; Huang and Chiu 2018).

In the present work, the mSim code capable of simulating two-dimensional sharp interface groundwater flow in porous media (Kourakos 2018) is used to simulate the seawater intrusion into coastal aquifers in Pavanje river basin of coastal Karnataka, India. The mSim toolbox is a script written in MATLAB primarily used with finite-element methods to simulate non-point source pollution in groundwater aquifers (Kourakos and Harter 2013; Mozafariet *et al.* 2018). The modelling approach, assumptions and justifications are described in detail in Kourakos *et al.* (2012) and Kourakos and Mantoglou (2013, 2015). In the current version of mSim, Gmsh is used to generate a 2D mesh only, and the 3D mesh is obtained by extruding the 2D mesh in the vertical direction within mSim. The graphical user interface (GUI) provides an advantage in terms of modelling flexibility as GUIs can be useful when geometries are relatively simple, and users have to interactively select only a few planes, which correspond to the boundary conditions. However, in realistic aquifer simulation, where boundaries may be consisting of hundreds of different planes, interactive selection becomes very inefficient.

The other objective of this work is to explore the ability of COMSOL for simulating saltwater intrusion (SWI) in fractured coastal aquifers. COMSOL is a comprehensive simulation software environment for a wide range of applications (COMSOL Multiphysics 2008a, b). It is a user-friendly tool that facilitates all the modelling steps (pre-processing, meshing, solving and post-processing). The primary advantage of COMSOL is that it easily allows the coupling of several physical processes together to include all the necessary factors for a complete model. COMSOL includes a module called 'Subsurface Flow' devoted to the simulation of fluids flow in saturated and variably saturated porous media (Kourakos 2018).

2. Study area

The study area is located around Surathkal and Mukka of the Dakshina Kannada district, Karnataka situated along India's west coast as shown in figure 1(a). The areal extent is about 8 km^2, and the area is surrounded by the Arabian Sea on the west and the seasonal tidal river Pavanje in the north and north-eastern part. The area is characterised by relatively flat near the coast with

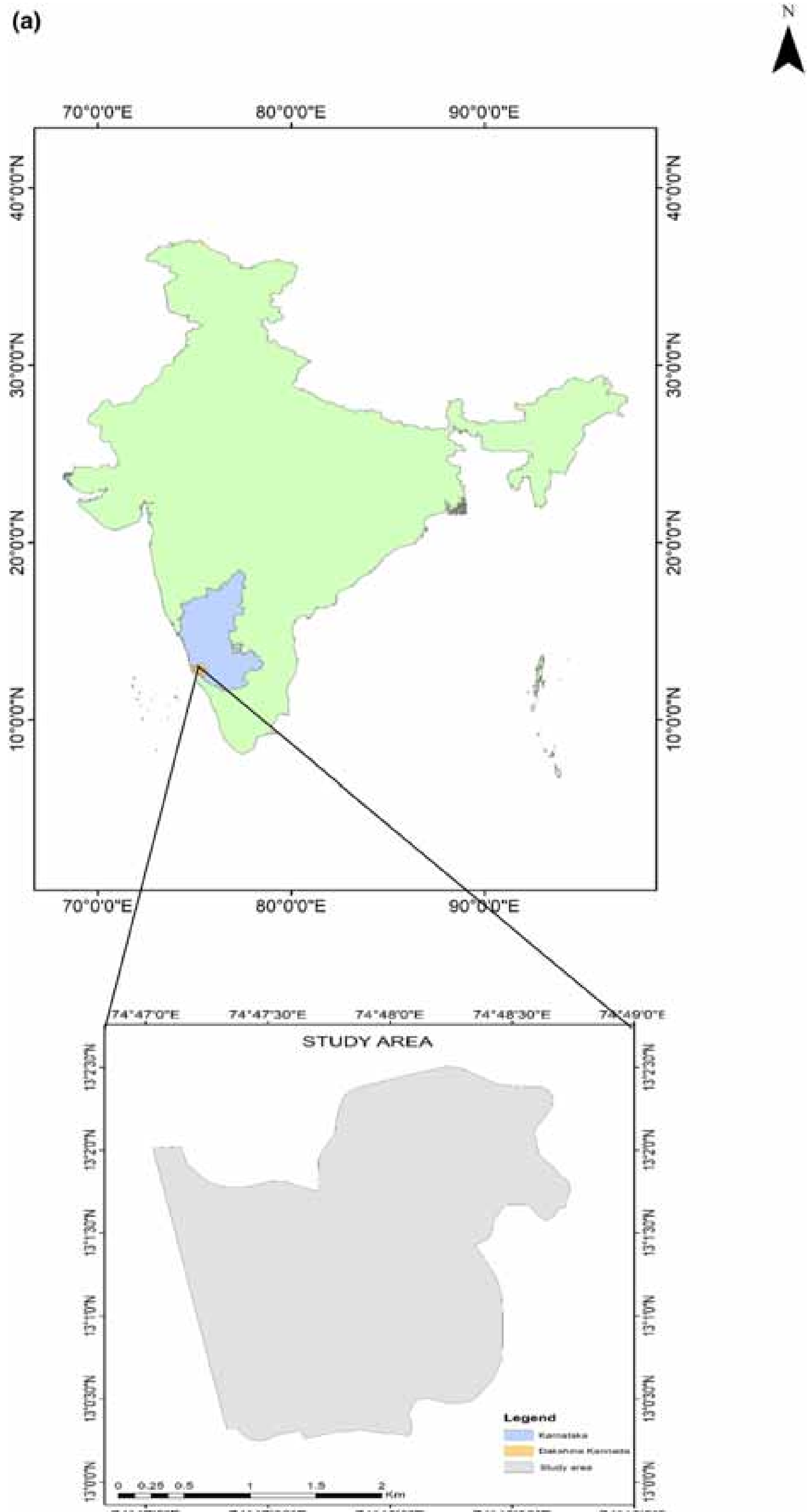

Figure 1. (**a**) Map of the study area. (**b**) Observation wells in the study area.

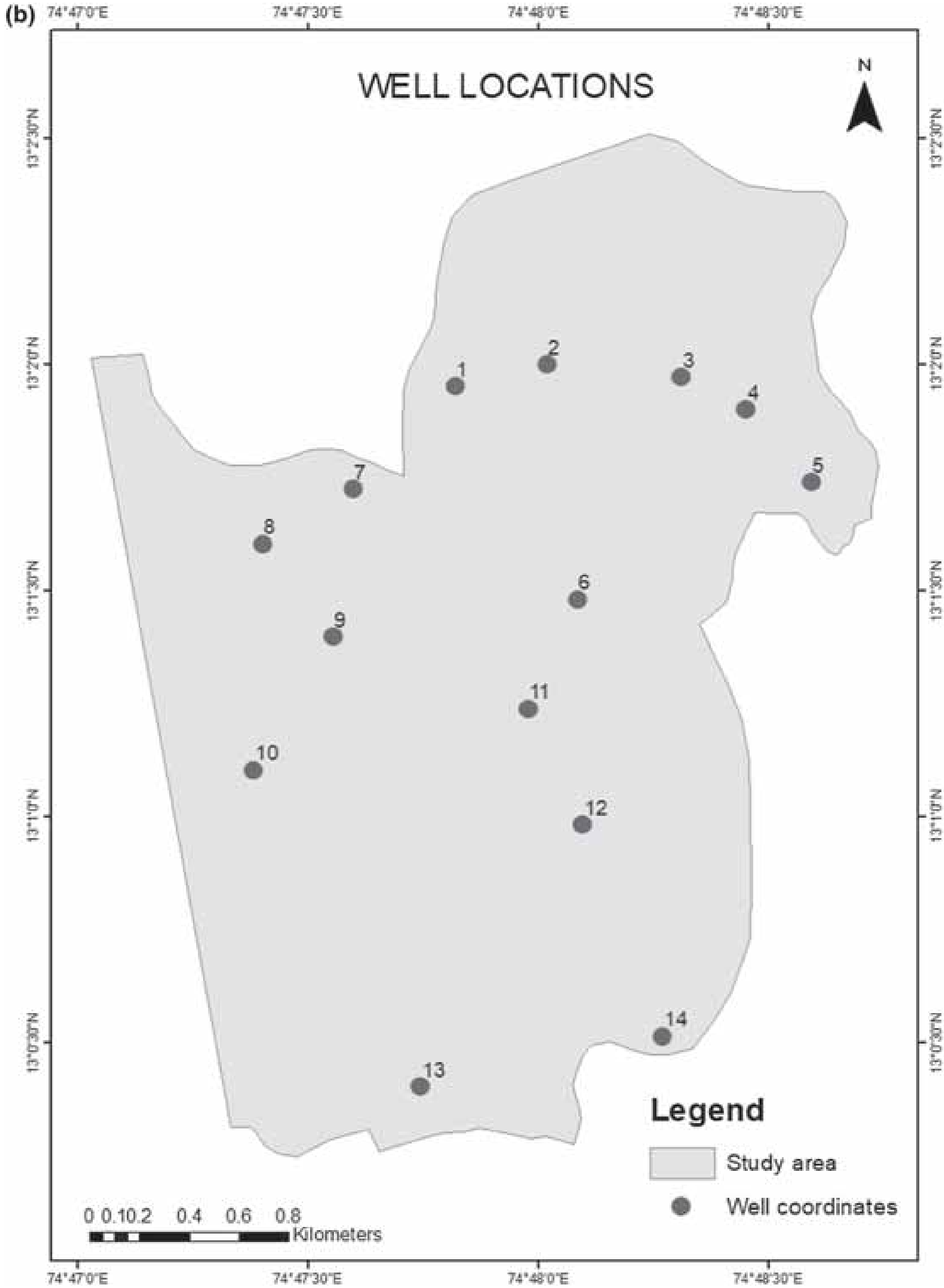

Figure 1. (*Continued.*)

undulating terrain inland with altitudes ranging up to 37 m above mean sea level (msl).

In addition to saltwater intrusion directly from the sea, it also intrudes into the river starting from October and reaches several kilometres upstream by the end of May contaminating the adjacent freshwater aquifers. Since Pavanje is a seasonal river, water demand for agriculture and domestic use is mainly met by groundwater during the non-monsoon period. This region falls under a humid tropical climate with an annual average rainfall of about 3797 mm of which approximately 87% is experienced during June to September. There are 14 observation wells (figure 1b) in the area which

Table 1. *Details of the observation wells.*

Well no.	Latitude	Longitude	Ground elevation above msl (m)	Well depth (m)
1	13°1′57″N	74°47′49.3″E	17	4.57
2	13°1′59.9″N	74°48′1.2″E	10	5.90
3	13°1′58.2″N	74°48′18.7″E	9	3.0
4	13°1′53.9″N	74°48′27.1″E	12	1.8
5	13°1′44.3″N	74°48′35.6″E	17	5.60
6	13°1′28.8″N	74°48′5.2″E	10	2.30
7	13°1′43.4″N	74°47′36″E	16	2.90
8	13°1′36.1″N	74°47′24.2″E	16	2.90
9	13°1′23.8″N	74°47′33.4″E	10	2.07
10	13°1′6.2″N	74°47′23.1″E	11	3.60
11	13°1′14.3″N	74°47′58.8″E	15	3.15
12	13°0′58.9″N	74°48′5.9″E	9	3.25
13	13°0′24.2″N	74°47′4.8″E	13	6.65
14	13°0′30.9″N	74°48′16.2″E	14	2.02

are well spread with one observation well for 1 km^2, except for the southwestern part which is barren. The details of the observation wells are given in table 1. The monthly water level and quality in these wells were monitored over 3 years, from 2005 to 2008 (Vyshali 2008).

3. Methodology

3.1 *Coastal aquifer modeling*

Flow in coastal aquifers is a very complex process due to mixing of two fluid phases and resulting fluid density depends on the unknown concentration (Cheng and Ouazar 1999). The extent of saltwater intrusion in coastal aquifers may be estimated by modelling flow in the aquifer as miscible or immiscible flow approaches. According to the immiscible flow model, the unconfined coastal aquifer is divided into two distinct zones. In the first zone (zone 1) the aquifer behaves as an unconfined one, while in the second zone (zone 2), a freshwater lens floats above the static saltwater wedge (figure 2). The steady state flow in the unconfined aquifer is governed by the following equation (Mantoglou *et al.* 2004):

$$\frac{\partial}{\partial x}\left(K\frac{\partial \Phi}{\partial x}\right)+\frac{\partial}{\partial y}\left(K\frac{\partial \Phi}{\partial y}\right)+N-Q(x,y)=0 \quad (1)$$

where ϕ = flow potential; K = aquifer's hydraulic conductivity; $Q(x, y)$ = total pumping rate; N = uniform recharge rate; x and y = coordinate axes. It should be noted that equation 1 is based on the single potential formulation and could be applied in both zones of the aquifer.

The total pumping rate could be expressed as:

$$Q(x,y)=\sum_{j=1}^{M} Qj\ \delta\left(x-x_{wj},\ y-y_{wj}\right) \quad (2)$$

where x_{wj}, y_{wj} = coordinates; Q_j = pumping rate of the jth well and δ = Dirac delta function. Groundwater abstraction data was collected from Lathashri and Mahesha (2015). And for each season it will vary accordingly. 875.04, 524.164 and 749.96 m^3/day are the groundwater draft considered for the pre-monsoon, monsoon and post-monsoon seasons, respectively.

The flow potential for the case of unconfined aquifers is defined as (Cheng and Ouazar 1999):

$$\Phi=\frac{1}{2}\left[h_f^2-(1+\varepsilon)\,\varepsilon^2\right],\quad \text{zone 1} \quad (3)$$

$$\Phi=\frac{(1+\varepsilon)}{2\varepsilon}\left(h_f-\varepsilon\right)^2,\quad \text{zone 2} \quad (4)$$

3.2 *Simulation of saltwater intrusion*

The benchmark involves migration of saltwater through a porous medium initially saturated with freshwater. The problem is simulated using a 2D model with triangular elements. The short terms responses from the software are of practical importance and hence, are also investigated in the analysis. COMSOL Multiphysics 5.3a software provides steady state solution to the problem.

The COMSOL Multiphysics is a great simulation software environment for a broad spectrum of applications and it has an interactive interface that facilitates the process of modelling and enables

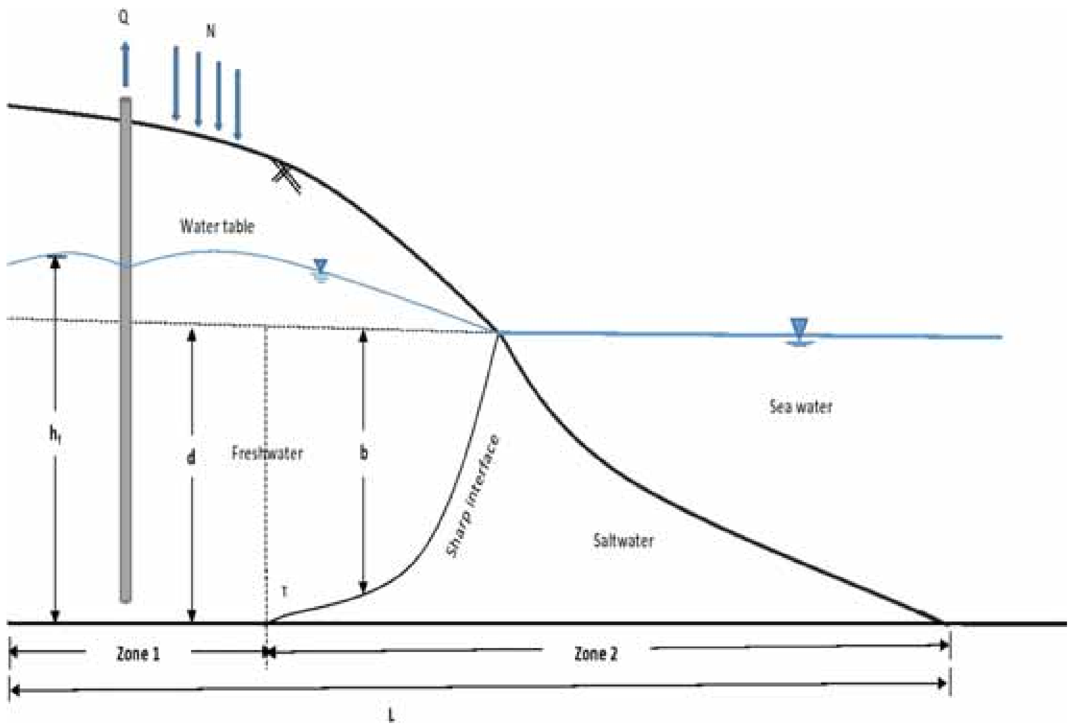

Figure 2. Vertical cross-section of an unconfined coastal aquifer based on the sharp interface approximation.

simple coupling of various physical procedures. The module Subsurface Flow (Kourakos 2018) expands the modelling environment of COMSOL to fluid flow applications. COMSOL is increasingly used in geophysical, hydrogeological and environmental phenomena inquiry. This software's user interface enables the modelling process, geometry definition, mesh generation, editing and coupling of PDE equations, solving, and post-processing efficiently. The COMSOL is also flexible in seaside circumstances with variable concentration limits.

As the summer advances, the water level declines as observed in almost all the wells. The salinity of the samples analysed (Vyshali *et al.* 2008) indicated that a few wells in the study area are vulnerable to saltwater intrusion. The benchmark involves migration of saline water through a porous medium initially saturated with freshwater. The model domain in DXF format is imported in to the software domain. A structured meshing is used which is similar to the mesh properties developed for flow simulation.

3.3 *Model development*

The first step in numerical modelling is to generate a mesh for the modelling domain into triangular elements. In this study, the domain is described by shapefiles. A few more fields are added which instruct Gmsh how to refine the mesh around the wells. The minimum element length near the wells is considered equal to 5 m and the maximum element length equal to 500 m at 1 m distance from the wells. By using mSim toolbox the finite element mesh is generated (figure 3). The mesh contains 1070 vertices with 2283 triangular elements. Although the mSim solves the partial differential equation of the groundwater flow, the result is obtained in terms of the potential Φ and is converted to hydraulic head on monthly basis.

The details about the observation wells and the water level data during the period February 2005 to January 2008 in the study area were collected from Vyshali (2008) and the elevation of each well with respect to mean sea level was established using the Google Earth (2004). The recharge is computed by multiplying the recharge coefficient of 10% of rainfall. According to the Groundwater Estimation committee (GEC 1997), for the west coast of India, recharge coefficient can be considered in the range of 8–12%. As the study area is a micro-basin, a uniform recharge rate is assumed. The hydraulic conductivity is considered to be spatially varied and the area is considered to be consisting of different zones of uniform hydraulic conductivity. The shape of the zones and their values are defined by the shapefile created in

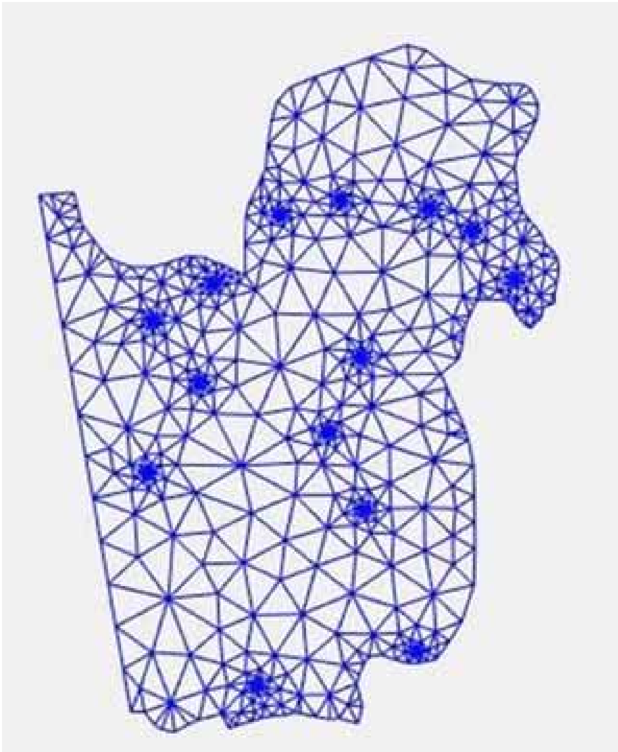

Figure 3. 2D Mesh generated by mSim.

ArcGIS as an input for the model. In this study, isotropic aquifer is considered.

The model executed for three seasons, i.e., summer (February–May), monsoon (June–September) and post-monsoon (October–January). For each season, discharge from wells varies depending on the demand variation (Lathashri and Mahesha 2015). Proper boundary conditions are incorporated as per problem definition. The west boundary is having constant head equal to 0 m (sea boundary). The north-east boundary has constant head equal to the maximum water level in Pavanje river (river boundary). The south-east side is considered to be impervious.

3.4 *Predictive simulation*

The present work explores the feasibility study on the effects of various stress scenarios on the aquifer by executing the numerical model. This study is taken up to investigate the response of the aquifer because of the likely increase in pumping rates and decreased recharge rates. The response is measured in terms of groundwater head and extent of saltwater intrusion. In the first scenario, the pumping rate for all the wells is increased uniformly by 50, 100, and 200%. The second scenario is planned for a 50% decrease as well as increase in recharge rate. In the third scenario, an increase in groundwater draft together with a decrease in recharge rate is considered. The fourth scenario considers sensitivity analysis on the decrease and increase of hydraulic conductivity by 50% of the initial value. The response of the aquifer system during the prediction is illustrated by representing comparative plots and graphs for water table elevation and groundwater salinity at a few locations in the study area.

4. Results and discussion

4.1 *Calibration and validation of model*

The model is calibrated for the period of 3 years (2005–2007). The optimum values of the parameters used in COMSOL after seasonal calibration are listed in table 2. The model efficiency values R^2, RMSE, r and Nash Sutcliffe efficiency (NSE) obtained after analysing the observed and simulated values at several observation wells are listed in table 3. There is a reasonable correlation between the simulated and observed groundwater data with statistics $R^2 = 0.67$ to 0.96 and NSE $\geq$ 0.5. The optimal hydraulic conductivity obtained after seasonal calibration is given in table 4 and the final optimal recharge coefficient obtained was 20% of rainfall excess.

It is essential to check the authenticity of the model before applying it for predictive scenario simulation through the validation process. The validation is carried out for one year during 2007–2008 subsequent to calibration run. A total of 14 wells are used for validation purpose. The R^2, RMSE, r and NSE values obtained are listed in table 5 after analysing the observed and simulated groundwater data at the observation wells. The results are found to be consistent with that of the calibration results and the model can be considered reliable for future predictions.

Table 2. *Optimal parameters used in COMSOL after seasonal calibration.*

Parameter	Value
Acceleration due to gravity (g, m/s^2)	9.81
Freshwater density (ρ_f, kg/m^3)	1000
Seawater density (ρ_s, kg/m^3)	1025
Freshwater concentration (c_0, mol/m^3)	0
Porosity (ε)	0.3
Viscosity (μ, kg/m/s)	0.0001
Permeability (k, m^2)	1.0204×10^{-9}
Freshwater inflow velocity (ν, m/s)	6.6×10^{-5}

Table 3. *Groundwater model efficiency values of each well after calibration during 2005–2007.*

Well no:	RMSE (m)	NSE	r	R^2
1	0.6522	0.5623	0.918	0.842
2	0.7424	0.348	0.8222	0.676
3	0.567	0.6988	0.8986	0.807
4	0.5522	0.6478	0.9008	0.811
5	0.4962	0.1646	0.843	0.71
6	0.6963	0.3735	0.8416	0.708
7	0.78955	0.402	0.9221	0.676
8	0.4587	0.7567	0.936	0.876
9	0.4088	0.7942	0.897	0.804
10	0.6965	0.6868	0.8708	0.758
11	0.6482	0.7475	0.9118	0.831
12	0.5828	0.9575	0.983	0.843
13	0.4576	0.6135	0.8578	0.966
14	0.4576	0.6135	0.8578	0.735

Table 4. *Optimal hydraulic conductivity values after seasonal calibration.*

Zone	Hydraulic conductivity value (m/d), kx = ky
1	12
2	20
3	28
4	10
5	16

Table 5. *Groundwater model efficiency values of each well during validation during 2007–2008.*

Well no.	RMSE (m)	NSE	R	R^2
1	0.616	0.533	0.749	0.561
2	0.2464	0.894	0.9624	0.926
3	0.3719	0.4294	0.7498	0.562
4	0.4029	0.6928	0.8386	0.72
5	0.2	0.8505	0.9326	0.869
6	0.5236	0.7029	0.874	0.763
7	0.4168	0.5832	0.8571	0.734
8	0.4739	0.6682	0.8601	0.739
9	0.1743	0.9173	0.9708	0.942
10	0.642	0.7953	0.9015	0.81
11	0.7512	0.6907	0.9	0.645
12	0.6444	0.1563	0.8034	0.602
13	0.5127	0.533	0.9818	0.964
14	0.3857	0.6917	0.9296	0.864

4.2 *Groundwater flow model*

The steady water table elevation was simulated on monthly basis. The water table hits the lowest level by the end of April (figure 4a) with more blue shade. The water table gets saturated during the monsoon season and water table during July is shown in figure 4(b). The water table declines gradually by the end of November (post-monsoon) (figure 4c). Majority of the wells (10) have significant variations (3–8 m), whereas, for some other wells (4 wells), the variation was within a couple of meters over the entire year. Well no. 13 shows drastic lowering of the water level from about 12 (monsoon) to 4 m (above mean sea level) during non-monsoon months. The driest period was observed to be the end of April since the area experiences the pre-monsoon showers during May.

4.3 *Saltwater intrusion model*

The results obtained from COMSOL Multiphysics 5.3-a, showed a salinity range of 0–20 mol/m^3. The standard limit of salinity of water for use is 3.5 mol/m^3. The wells 4, 7, 11 and 12 are having salinity more than 5 mol/m^3 and are very severely affected by saltwater intrusion due to proximity to the sea. The above wells are also located in the low lying areas. Wells 13 and 14 which are at a distance of 724 and 1690 m, respectively from the sea are not affected by salinity severely. But well number 7 as shown in figure 5 is consistently showing higher salinity (more than 5 mol/m^3) throughout the year. This well is 887 m away from the sea coast. Well number 11 turns saline only during the summer season (March–May). All the other wells have salinity within 3.5 mol/m^3.

Figure 6(a, b and c) shows salinity distribution over the region during the end of January, April and June, respectively. The minimum salinity is during the monsoon season and starts increasing thereafter in the area till the end of summer. However, for most of the years, the salinity during May is slightly less than April, may be due to the pre-monsoon showers during May. The salinity observed in May 2006, 2007 shows lower values compared to 2005 values due to significant pre-monsoon showers occurred in the region during those years.

4.4 *Predictive simulation – groundwater flow*

After satisfactory performance, the models are applied for simulating the future anticipated development scenarios which consider increase in groundwater draft, varied recharge rate owing to changes in the precipitation and sensitivity analysis related to hydraulic conductivity.

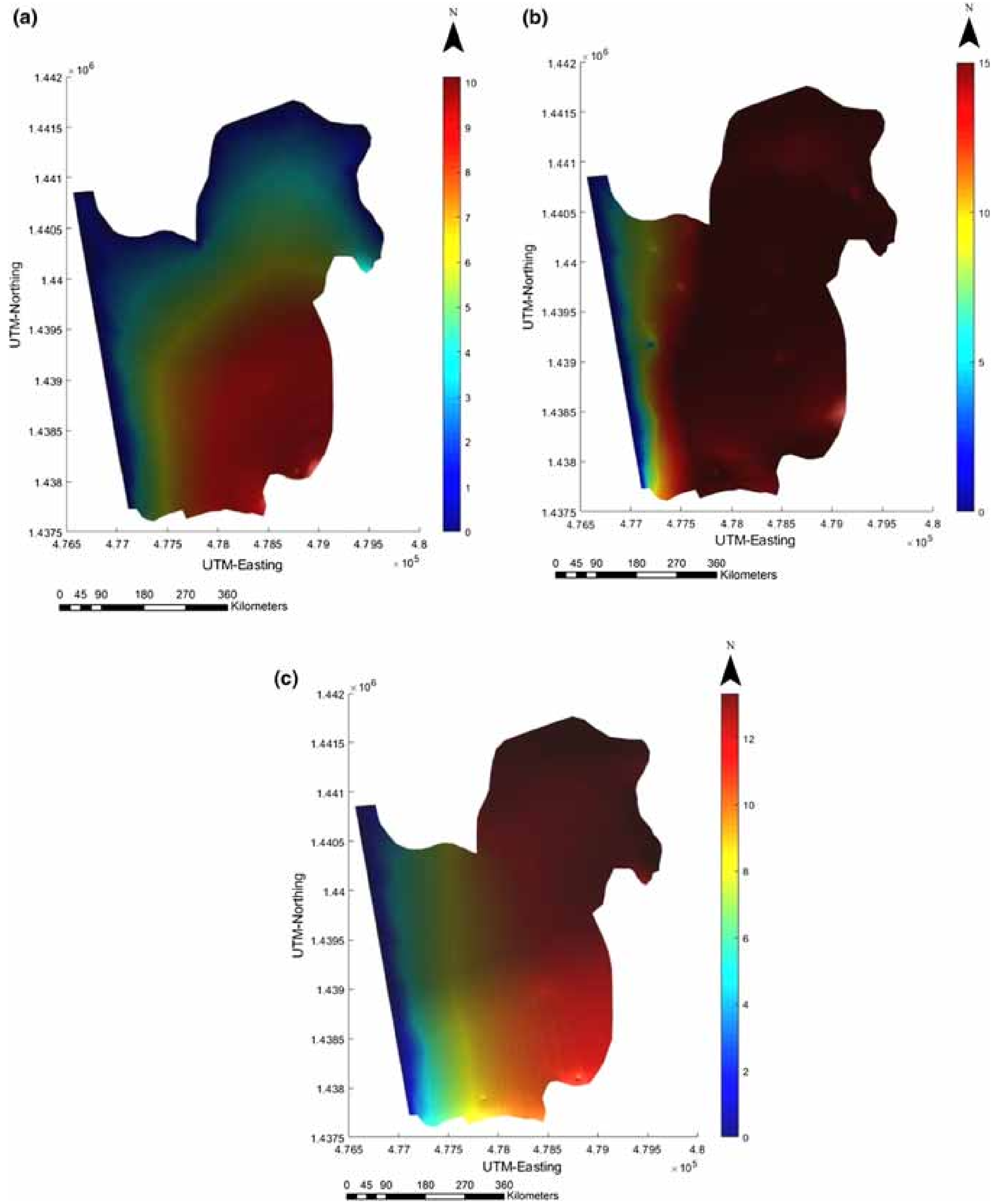

Figure 4. (**a**) Hydraulic head above mean sea level by the end of April. (**b**) Hydraulic head above mean sea level by the end of July. (**c**) Hydraulic head above mean sea level by the end of November.

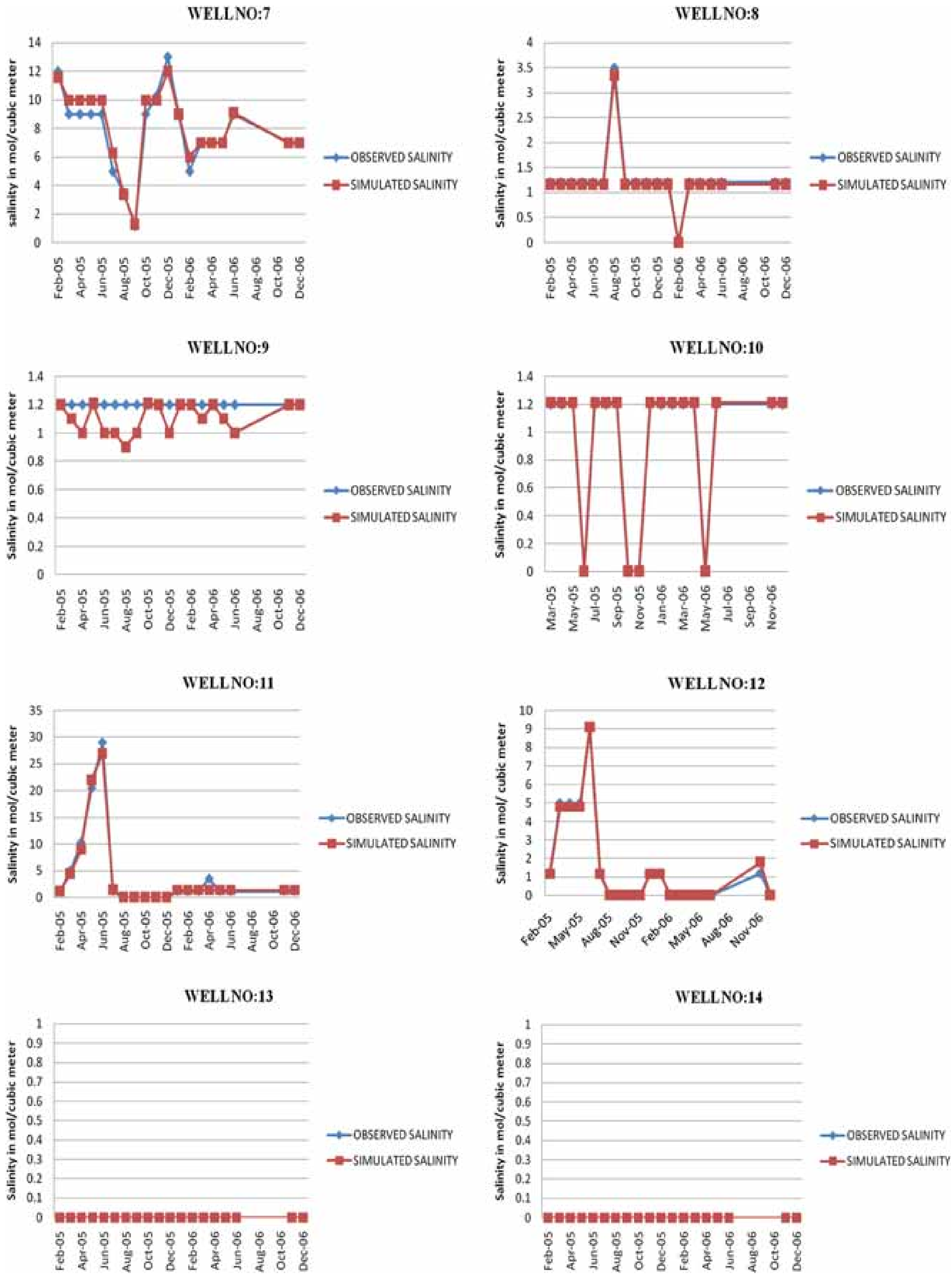

Figure 5. Observed vs. simulated salinity for Well No. 7–14 respectively.

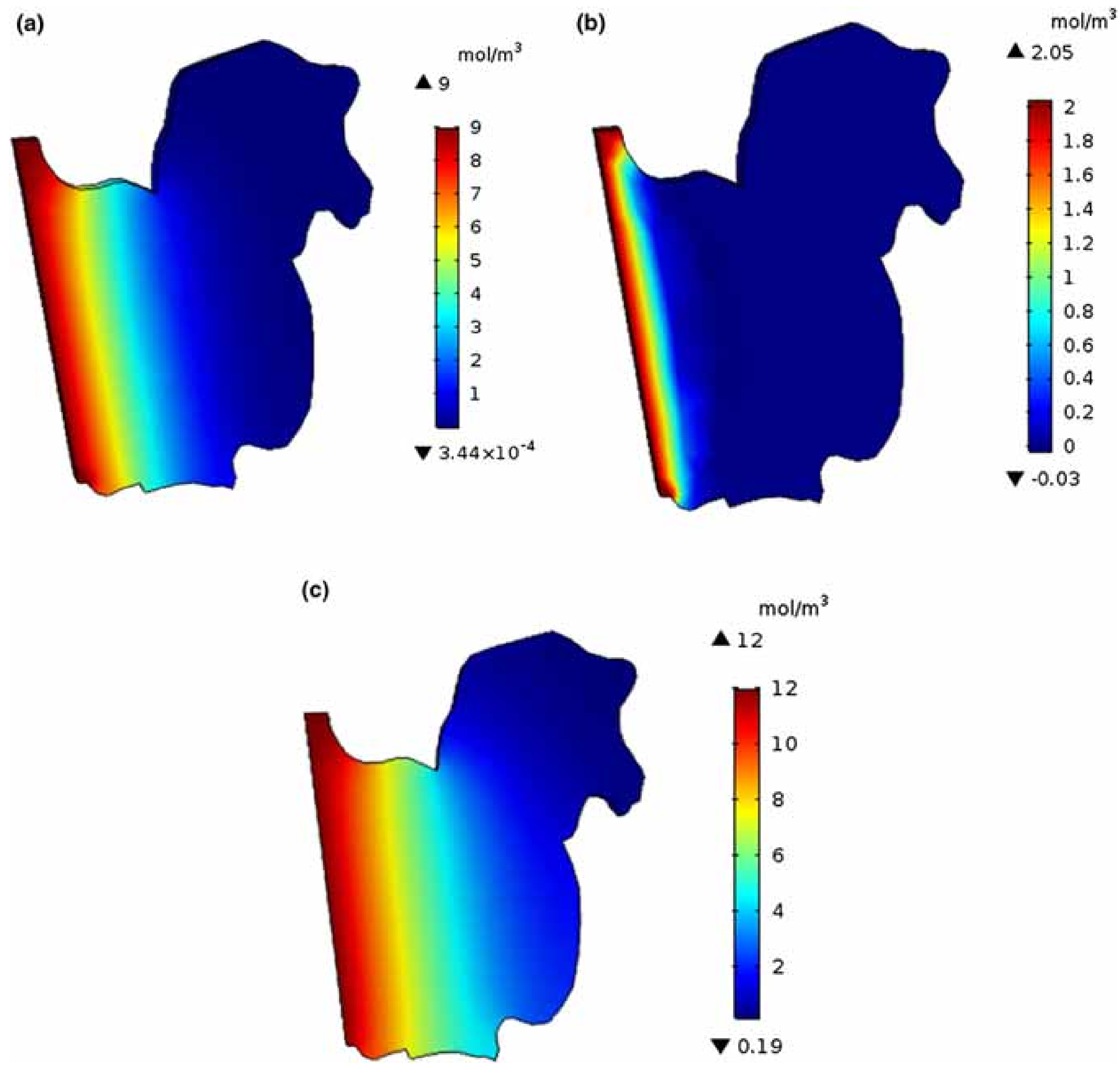

Figure 6. (**a**) Saltwater intrusion during January (post-monsoon season). (**b**) Saltwater intrusion during end of June (monsoon season). (**c**) Saltwater intrusion during end of April (pre-monsoon season).

***Scenario* 1:** If the groundwater draft is increased by 50%, the available groundwater head during the monsoon is almost unaffected. The minimum head (summer) available ranges from zero to −5 m. If the groundwater draft is increased by 100%, the groundwater head during monsoon reduces by 4–5 m. Some wells show negative head as well. If the groundwater draft is further increased, i.e., by 200%, the total available groundwater head during the monsoon drastically reduces and reaches the mean sea level. During the pre-monsoon season, negative groundwater head along the coast as well as low lying areas (river line) were observed. The post-monsoon season was worst affected by the increase in groundwater draft. Here the maximum available head is restricted to mean sea level along the coastal areas, and rest of the region shows the negative head.

***Scenario* 2:** The maximum head available during the monsoon becomes double if the recharge rate is increased by 50% of the initial value. During the post-monsoon season, the maximum head available increases by only 1–2 m since the groundwater table depletes after the monsoon rains. The summer groundwater table is not getting affected by the increase of recharge since rainfall is scanty during this season.

***Scenario* 3:** The critical condition that can occur to an aquifer system is decrease in ground water recharge combined with an increase in groundwater draft. The maximum head in the study area gets reduced by 5–6 m and most of the area having head value between −1 and 6 m. During the post-monsoon season, the minimum head available reduces to 1 m below msl. In case of pre-monsoon season, over 90% of the area, water table drops below the msl. The water table elevation during for the monsoon, pre-monsoon and post-monsoon seasons are represented in figure 7(a, b, c), respectively.

***Scenario* 4:** This scenario is considered for the sensitivity analysis purpose only since, aquifer parameters do not vary significantly over the period of time. If hydraulic conductivity gets reduced by 50% of the initial value, the minimum head available during the monsoon season will become 5 m below the msl which is less compared to normal hydraulic conductivity scenario. The pre-monsoon season water table does not get affected by an increase or decrease in hydraulic conductivity since the quantity of water available is small. But, during the post-monsoon season, the range of water table elevation is short, i.e., from 0 to −1 m.

4.5 *Predictive simulation – salinity*

***Scenario* 1:** Increase in groundwater draft itself can result in rise in salinity intrusion to the coastal aquifer region to a large extent. Compared to the initial value of saltwater concentration, the salinity of the aquifer is increased by 2–3 mol/m^3 due to the excessive groundwater draft (200% of initial draft). The areal extent of saltwater intrusion in this case was found to be about 500 m from the sea or tidal river carrying sea water.

***Scenario* 2:** Reduced recharge rate makes the aquifer more susceptible to the inland movement of saltwater. Here, aquifer along the sea coast is safe from the salinity only during the monsoon season (<3.5 mol/m^3). When compared to the pre-monsoon season, the post-monsoon has higher concentration and distribution may be due to increased groundwater draft for irrigation. Decrease in recharge by 50% could cause increase in saltwater concentration by 1–2 mol/m^3. The effect of increase in recharge rate up to 50% has negligible effect on salinity intrusion.

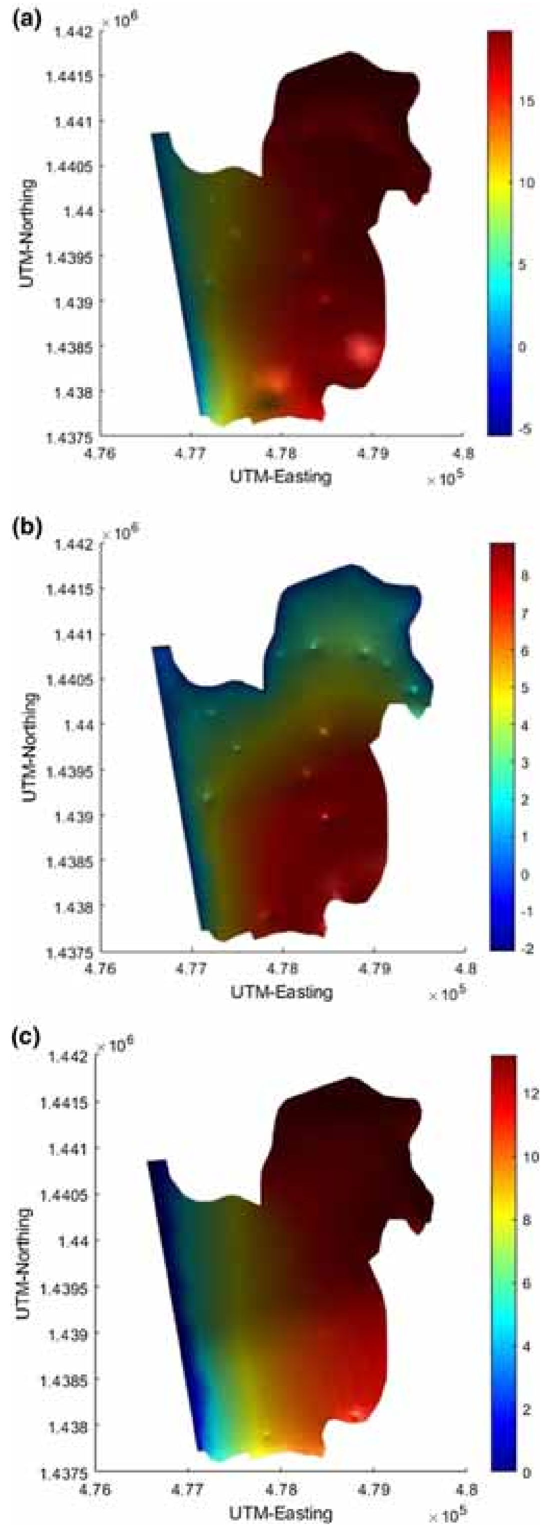

Figure 7. Impacts on water table when groundwater recharge decreases by 50% and GW draft increases by 200% during monsoon (**a**), pre-monsoon (**b**) and post-monsoon (**c**) seasons respectively.

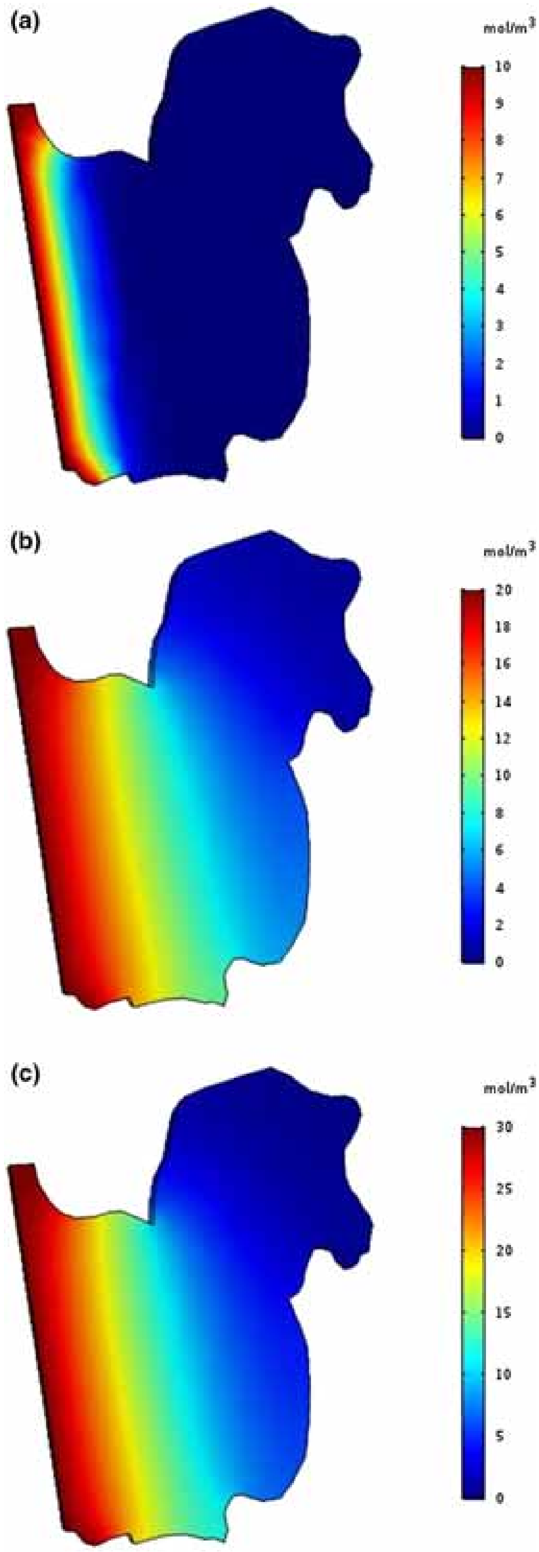

Figure 8. Spatial distribution of salinity for scenario 4 case 50% reduction in ground water recharge along with 200% increase in GW draft for the monsoon (**a**), pre-monsoon (**b**) and post-monsoon (**c**) seasons respectively.

***Scenario* 3:** The study reveals that, the worst combination of reduced recharge rate with increased groundwater draft has a serious impact on the aquifer system in terms of saltwater intrusion. Figure 8(a, b, c) represents saltwater intrusion scenarios during the monsoon, pre-monsoon and post-monsoon seasons, respectively. In this case, the saltwater intrudes more than 5 mol/m^3 rendering 25% of the aquifer water unsuitable for drinking. The total salinity along the seacoast becomes more than double if this situation prevails.

***Scenario* 4:** The hydraulic conductivity was found to be directly proportional to saltwater intrusion and increase in hydraulic conductivity by 50%, increases saltwater intrusion up to 4 mol/m^3 during the monsoon season. Generally, we can say that 50% increase in hydraulic conductivity can cause 15–18% increase in saltwater intrusion. A decrease in hydraulic conductivity reduces saltwater intrusion to some extent. When compared to the initial conditions, a decrease in saltwater intrusion is visible for all the seasons except the monsoon season.

5. Conclusions

The numerical groundwater simulation using mSim and COMSOL multiphysics carried out for an adequate and efficient assessment of groundwater resources in a tropical, coastal aquifer under steady state condition. The study is focussed on a shallow, lateritic, unconfined aquifer, with good groundwater potential. The salient features of the investigation are as follows:

- The model was calibrated and validated for groundwater flow and salinity distribution with the observed data. The calibration results indicate that, there exists a reasonable correlation ($R^2 = 0.67$ to 0.96) between the simulated and observed water levels. The RMSE, r and NSE values also follow the same tendency. The model was also calibrated for salinity with the ability to simulate salinity reasonably good with NSE $\geq$ 0.5. The model was performing better during the different seasons. The validation results also indicate a reasonable simulation by the model.
- The water table variation over the years in the region was found to be quite significant (about 3–12 m). The water table reaches its saturation level by the end of the monsoon season every year.
- The wells 4, 7, 11 and 12 in Pavanje river basin were found to be having the salinity exceeding

the standard limit of 3.5 mol/m^3 during the post-monsoon and the summer seasons. The well no. 7 was found to be saline throughout the year.

- The management of fresh water table in the range 1–1.5 m above the mean sea level is of prime importance for the sustainability against seawater intrusion.
- The post-monsoon season water table would be worst affected if the groundwater draft gets increased to 2–3 times of the present value.
- The variation of recharge during the post-monsoon has no effect since rainfall is relatively less during this season compared to the monsoon season.
- More than 90% of the area during the post-monsoon season falls below the mean sea level due to steep increase in groundwater draft (200% of the present withdrawal rate) coupled with 50% decrease in recharge rate. This is a very critical condition that can occur to an aquifer system which could result in aggressive saltwater intrusion.
- The aquifer near the seacoast is safe from salinity during the monsoon season (salinity $<$3.5 mol/m^3). It can be concluded that, increase in natural surface recharge up to 50% has no controlling effect on saltwater intrusion.
- The worst combination of reduced recharge rate with increase pumping rates renders 25% of the aquifer water unsuitable for drinking. The total salinity of the aquifer may be more than double if this situation prevails.
- The impact of hydraulic conductivity was found to be affecting saltwater intrusion. An increase in hydraulic conductivity by 50% would cause 15–18% increase in saltwater intrusion.

The results may give useful insights into the coastal processes and river–aquifer interactions with quantitative estimates of fresh water and saltwater intrusion.

Acknowledgement

The authors are grateful to Dr. George Kourakos for introducing mSim as a precursor to contaminant transport modelling.

References

Bobba A G 2012 Ground water-surface water interface (GWSWI) modelling: Recent advances and future challenges; *Water Resour. Manag.* **26(14)** 4105–4131.

Cheng A H D and Ouazar D 1999 *Analytical Solutions*; In: Seawater Intrusion in Coastal Aquifers – Concepts, Methods and Practices. Theory and Applications of Transport in Porous Media (eds) Bear J, Cheng A H D, Sorek S, Ouazar D and Herrera I, Vol. 14, Springer, Dordrecht.

COMSOL Multiphysics 2008a *COMSOL Installation and Operations Guide: Version 3.5.* Stockholm: COMSOL AB.

COMSOL Multiphysics 2008b *COMSOL Multiphysics Modeling Guide: Version 3.5* Stockholm: COMSOL AB.

Essink G O 2001 Improving fresh groundwater supply: problems and solutions; *Ocean Coast. Manag.* **44** 429–449.

GEC 1997 Groundwater Resource Estimation Methodology; Report of the Groundwater Resource Estimation Committee, Ministry of Water Resources, Government of India, New Delhi.

Google Earth 2004 Virtual globe. http://www.googleearth.com.

Huang P S and Chiu Y C 2018 A simulation-optimization model for seawater intrusion management at Pingtung coastal area Taiwan; *Water* **10** 251.

Kourakos G 2018 Subsurface; http://subsurface.gr/software/msim/.

Kourakos G and Mantoglou A 2013 Development of a multi-objective optimization algorithm using surrogate models for coastal aquifer management; *J. Hydrol.* **479** 13–23.

Kourakos G, Klein F, Cortis A and Harter T 2012 A groundwater nonpoint source pollution modeling framework to evaluate long-term dynamics of pollutant exceedance probabilities in wells and other discharge locations; *Water Resour. Res.* **48** W00L13, https://doi.org/10.1029/2011WR010813.

Kourakos G and Mantoglou A 2015 An efficient simulation–optimization coupling for management of coastal aquifers; *Hydrogeol. J.* **23** 1167–1179.

Kourakos G and Harter T 2013 Vectorized simulation of groundwater flow and streamline transport; *Environ. Model. Softw.* **52** 207–221.

Lathashri U A and Mahesha A 2015 Predictive simulation of seawater intrusion in a tropical coastal aquifer; *J. Environ. Eng. ASCE.* **142** D4015001. https://doi.org/10.1061/(asce)ee.1943-7870.0001037.

Lin J, Snodsmith J B, Zheng C and Wu J 2009 A modelling study of seawater intrusion in Alabama Gulf Coast, USA; *Environ. Geol.* **57** 119–130.

Mantoglou A 2003 Pumping management of coastal aquifers using analytical models of saltwater intrusion; *Water Resour. Res.* **39** 1335.

Mantoglou A, Papantoniou M and Giannoulopoulos P 2004 Management of coastal aquifers based on nonlinear optimization and evolutionary algorithms; *J. Hydrol.* **287** 209–228. https://doi.org/10.1016/j.jhydrol.2004.04.011

Mozafari B, Fahs M, Ashtiani, A B, Simmons C T and Younes R 2018 On the use of COMSOL multiphysics for seawater intrusion in fractured coastal aquifers; 25th Salt Water Intrusion Meeting (SWIM 2018) Gdańsk Poland (eds) Szymkiewicz A, Sadurski A, Jaworska-Szulc B, *Web of Conferences* **54** 00020.

Priyanka B N, Mohan Kumar M S and Mahesha A 2018 Estimating anisotropic heterogeneous hydraulic conductivity and dispersivity in a layered coastal aquifer of Dakshina Kannada district, Karnataka; *J. Hydrol.* **565** 302–317.

Vyshali, Palchaudhury M and Mahesha A 2008 Simulation of saltwater intrusion in the Pavanje–Gurpur basins of Karnataka; *ISH J. Hydraul. Eng.* **14(2)** 49–60.

Vyshali 2008 Studies on saltwater intrusion in the coastal DK district, Karnataka; PhD thesis, Dept. of Applied Mechanics and Hydraulics, National Institute of Technology Karnataka, Surathkal, Mangalore, India, pp. 52–72.

Werner A D 2010 A review of seawater intrusion and its management in Australia; *Hydrogeol. J.* **18** 281–285.

Corresponding editor: Subimal Ghosh